Songklanakarin J. Sci. Technol.
47 (3), 214–220, May – Jun. 2025

http://www.sjst.psu.ac.th

Original Article

Evaluation of the trends and variability of extreme temperatures in the Sumatra region

Suhadi*, Jamiatul Khairunnisa Putri, Herma Widya, and Tazkia Hayati

Physics Education Study Program, Universitas Islam Negeri Raden Fatah Palembang, Palembang, 30126 Indonesia

Received: 11 September 2024; Revised: 8 January 2025; Accepted: 21 April 2025

Abstract

Extreme temperatures, in particular, which are an indicator of climate change, are currently a serious concern for various parties in the world. This concern extends beyond the daily impact, as it also pertains to sustainable living. Using ERA5 surface temperature data for 30 years (1994-2023), we evaluate the trend and variability of extreme temperatures in Sumatra, with the Focus of Location (FoL) being Palembang (UIN Raden Fatah Palembang), South Sumatra. We assessed the trends and variability of extreme Temperatures using the Mann-Kendal test and Empirical Orthogonal Function (EOF) methods. The research results showed that TXx, TXn, and TNx experienced a significant increase of 0.1°C each year, while TNn experienced an increase of 0.3°C each year. The extreme temperature variability shown in EOF2 is greater than that in EOF1. EOF2 also shows that warmer extreme temperatures occur in southern Sumatra, including FoL. In addition, peak PC2 amplitude was detected during the ENSO and IOD (El Niño and positive IOD) periods.

Keywords: trend, variability, extreme temperature, UIN Raden Fatah Palembang, south Sumatra, Indonesia, Mann-Kendal test, empirical orthogonal function (EOF)

1. Introduction

Temperatures are an indicator of climate change, which is a serious concern worldwide, especially among academics. In connection with this climate change, the Intergovernmental Panel on Climate Change (IPCC) shows that global temperatures have increased by 0.85°C since 2012 (IPCC, 2012, 2018). Researchers in several countries, including Indonesia, have confirmed this temperature rise. Khoir *et al.* (2018) showed that Jakarta City (Indonesia) experienced an extreme temperature rise in the period 1986-2014. Even the city's temperatures in 2050 and 2100 are predicted to be 28.5°C and 29.23°C (Subarna, 2017). Moreover, Supari *et al.* (2017) indicate that Indonesia is experiencing increases in day and night temperatures of 0.18 °C and 0.30 °C every decade. Akbar and Lubis (2022) suggest that this temperature rise is primarily due to human activity in Bengkulu city. Researchers from Australia (Dittus, Karoly, Donat, Lewis, & Alexander, 2018) show that annual extreme temperature variability is linked to sea surface temperature activity. Furthermore, extreme temperature rises are also happening in China, which has an impact on the local agricultural sector (Nie *et al.*, 2019).

Evaluation of extreme temperatures can be carried out using various methods, including General Extreme Value (GEV) (An *et al.*, 2020; Feng, Tipton, Xia, & Chang, 2019; Stott *et al.*, 2016). In addition, extreme temperatures can be evaluated using indices defined by the Expert Team on Climate Change Detection and Indices (ETCCDI). The ETCDDI temperature index determines various extreme daily temperature conditions, including those shown in Table 1. These various indices have been used by researchers, including those mentioned previously. This research was conducted by Chaney *et al.* (2014), who evaluated extreme climates in sub-Saharan Africa. In addition, Felix *et al.* (2021) also used an index based on ETCDDI to evaluate extreme temperatures in South Korea. Apart from being used by many researchers, the ETCDDI index is easier to apply than the GEV.

Some of the research that has been mentioned illustrates that extreme temperatures are a pertinent study today, especially with regard to sustainable living. Apart from updating extreme temperature data and information in

*Corresponding author
Email address: suhadi@radenfatah.ac.id

Table 1. Extreme temperature indexes used in the research.

No	ID	Indicator name	Definitions	Units
1	TXx	Max Tmax	Monthly maximum value of daily maxi mum temperature	°C
2	TXn	Max Tmin	Monthly minimum value of daily maximum temperature	°C
3	TNx	Min Tmax	Monthly maximum value of daily minimum temperature	°C
4	TNn	Min Tmin	Monthly minimum value of daily minimum temperature	°C
5	DTR	Diurnal temperature range	Monthly mean difference between TX and TN	°C

Indonesia, the Focus of Location (FoL) research was carried out in the Palembang area, South Sumatra, Indonesia. In addition, the Mann-Kendal method was used in the analysis of extreme temperature trends in similar research conducted in Indonesia. We then incorporated the Empirical Orthogonal Function (EOF) method and the Fourier transformation to observe the variability and peak periods of these temperatures. EOF itself is a very reliable method for determining the variability of the distribution of data and has been widely used in the field of meteorology (Iskandar, Sari, Setiabudiday, Yustian, & Monger, 2017). The findings can be used as a basis for determining policies, particularly disaster mitigation in various sectors related to extreme temperatures.

2. Materials and Methods

2.1 Data

This study uses the daily temperature data recorded over 30 years (1994–2023) at the Stasiun Klimatologi SUMSEL and Stasiun Meteorologi SMB II. Prior to data utilization, completeness was verified to ensure reliability. Quality control procedures were conducted to validate the consistency of maximum and minimum temperature records, ensuring that no minimum temperature exceeded the corresponding maximum temperature. Additionally, hourly ERA5 data with a spatial resolution of 0.25° was utilized to support broader spatial analyses, with a particular focus on the island of Sumatra and its surrounding areas.

The study occurred in the Sumatra region, specifically at UIN Raden Fatah Palembang campuses A, B, and C, as depicted in Figure 1. Furthermore, we utilized the Stasiun Klimatologi SUMSEL (D) and the Stasiun Meteorologi SMB II (E). We selected focus locations A, B, and C to implement the UIN Raden Fatah Palembang green campus program, demonstrating our commitment to global issues, particularly the extreme climate. Projection of temperature data (U) at locations A, B, and C from daily BMKG data using the Inverse Distance Weight technique (IDW).

$$U = \frac{\sum_{i=1}^{n} w_i(x,y)u_i}{\sum_{i=1}^{n} w_i(x,y)}, \quad (1)$$

$$w_i(x,y) = \frac{1}{\sqrt{(x-x_i)^2 + (y-y_i)^2}}, \quad (2)$$

u_i is the temperature on the longitude (x_i) and the latitude (y_i) to the i temperature data of the BMKG station. x and y are the length and latitude of locations A, B, and C. The subsequent five locations (A, B, C, D, and E) are named the Focus of Locations (FoL).

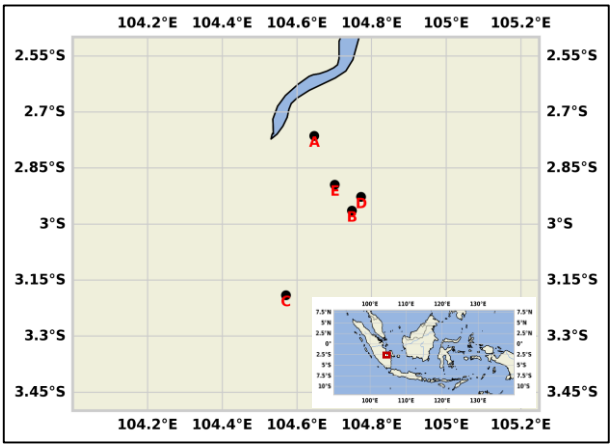

Figure 1. Area of Interest of the study

2.1 Methods

Extreme temperature examination is based on an index presented by the ETCCDI (Zhang, Feng, & Chan, 2018). There are 27 indices defined, but the study uses only the five shown in Table 1.

Akhsan *et al.* (2023); Akhsan *et al.* (2022); and Supari *et al.* (2017) defined TXx and TXn as the hottest and coldest temperatures during the day, while TNx and TNn were the hottest and coldest temperatures at night, respectively. Daily maximum (TX) and minimum (TN) temperatures from hourly ERA5 data are defined as the highest and lowest temperatures recorded within a day.

Examination of the trend of each index applied the Mann-Kendal (MK) test

$$Z_s = \begin{cases} \frac{S-1}{\sqrt{VAR(S)}}; & \text{if } S > 0 \\ 0 \quad ; & \text{if } S = 0 \\ \frac{S+1}{\sqrt{VAR(S)}}; & \text{if } S < 0 \end{cases} \quad (3)$$

with

$$VAR(S) = \frac{n(n-1)(2n+5)}{18}, \quad (4)$$

$$S = \sum_{i=1}^{n-1} \sum_{j=i+1}^{n} \operatorname{sgn}(X_j - X_i) \quad (5)$$

$$\operatorname{sgn}(X_j - X_i) = \begin{cases} +1\,; & \text{if } (X_j - X_i) > 0 \\ 0\,; & \text{if } (X_j - X_i) = 0 \\ -1\,; & \text{if } (X_j - X_i) < 0 \end{cases} \quad (6)$$

Gradients of this tendency are determined by

$$Q_i = \begin{cases} T_{\frac{n+1}{2}} & ;\text{for } n \text{ odd} \\ \frac{1}{2}\left(T_{\frac{n}{2}} + T_{\frac{n+2}{2}}\right) & ;\text{ for } n \text{ even} \end{cases} \quad (7)$$

with

$$T_n = \frac{X_j - X_k}{j - k} \quad (8)$$

for $n = 1,2,3, \ldots, n$; and X is the value of each index.

After computing the trend of extreme temperature, we evaluate the extreme temperature (TXx, TXn, TNx, TNn, DTR) variability using the EOF method. We use EOF to separate space-time-dimensional data into several orthogonal modes with maximum variance (Hannachi, Jolliffe, & Stephenson, 2007). Furthermore, in each EOF mode, we obtain a principal component (PC), which characterizes the low elevation of the EOF signal at a specific time. Technically, we can perform this EOF calculation using the Singular Value Decomposition method (SVD). For instance, given dimensional spatial-time temperature data *X*(*s*,*t*),

$$X(s,t) = \begin{bmatrix} x_{11} & \cdots & x_{1t} \\ \vdots & \ddots & \vdots \\ x_{s1} & \cdots & x_{st} \end{bmatrix} \quad (9)$$

The data matrix is shaped in such a way that it becomes a matrix with $Rank(r) = r$. Next is the decomposition.

$$SVD(X) = \sum_{i=1}^{r} U_i \Lambda_i V_i \quad (10)$$

The EOF and eigenvalues of the *i-th* mode are represented by U_i and Λ_i. We obtain the PC by multiplying each eigenvalue with the original data.

$$PC_i = (\Lambda_i)^T X \quad (11)$$

The details of this EOF method can be seen in (Antonio & Valeria, 2010; Hannachi *et al.* 2007). In order to determine the peak period of the PC, we transform this using the Fast Fourier Transform (FFT).

3. Results and Discussion

3.1 The extreme temperature trend

The results of extreme temperature calculations are shown in Figure 2. Throughout the 1994-2023 period, the extreme temperature trend shows a significant increase except for DTR. For 30 years TXx (Figure 2A), TXn (Figure 2B), TNx (Figure 2C.) and TNn (Figure 2D) respectively show an increasing trend of 0.0036°C/month, 0.0031°C/month, 0.0034 °C/month, and 0.0093°C/month or around 0.1°C, 0.1°C, 0.1°C and 0.3°C each year. This condition indicates that the weather is getting hotter, especially at night. This condition has also been demonstrated by Supari *et al.* (2017), who reported trends in maximum and minimum temperatures at FoL of 0.3°C per decade and 0.6°C per decade, respectively. Furthermore, Supari *et al.* (2017) confirmed the intensification of extreme temperature trends, attributing these changes to the influence of the strong 1997/1998 and moderate 2009/2010 El Niño events. The results of this research show that Indonesia experiences an increase in maximum daytime and nighttime temperatures of 0.24°C and 0.33°C, respectively, every decade. Apart from that, research conducted by Choi *et al.* (2009) in Malaysia showed results that were not much different, likewise with the results of research conducted by Limjirakan and Limsakul (2012) in Thailand.

Apart from that, an increase in temperature can also be seen based on the difference in maximum and minimum temperatures at the beginning and end of the observation period. At the beginning of the observation (1994-01-01), the average TXx and TXn were 32.2°C and 27.5°C respectively, whereas the average TNx and TNn at the end of the observation (2023-12-31), respectively, were 26.3°C and 23.4°C. This difference shows that the hottest nighttime temperature today (2023-12-31) is almost the same as the coldest daytime temperature 30 years ago (1994-01-01). This average extreme temperature is almost the same as the results of previous research conducted by Akhsan *et al.* (2022). The same researchers confirmed that the increase in extreme temperatures is predominantly correlated with ENSO and IOD (Akhsan *et al.* 2023). The increase in temperature in the neighboring city (Bengkulu) shown by Akbar & Lubis, (2022) is predominantly caused by human activity. Therefore, this increase in extreme temperatures can also be caused by the same thing.

Another finding of TNx (Figure 2C) in 1994-1999 and TNn (Figure 2D) in 2004-2009 by using IDW technique are look like insufficiently valid at the UIN RF B location. These results are due to the IDW technique used, and also due to the relatively large data differences between the Stasiun Klimatologi SUMSEL and Stasiun Meteorologi SMB II.

3.2 The variability of extreme temperature

We use EOF analysis to see variability in a wider area, especially on the island of Sumatra and its surroundings. However, prior to proceeding, the average temperature extremes, as shown in Figure 3, will be examined. The average maximum and minimum temperatures during the day and night (Figure 3.A-D) show suitability (mean TXx>TXn>TNx>TNn). The averages of TXx, TXn, TNx, and TNn ranged within 28.58°C-31.71°C, 25.45°C-28.58°C, 17.63°C-25.45°C, and 9.81°C-23.89°C, respectively. Meanwhile, the average DTR ranges from 1.98°C to 9.81°C. Each extreme temperature appears to be lower along the west coast of Sumatra island. This is natural because the elevation in this area is higher than on the eastern coast. FoL is located in an area where extreme temperatures (TXx, TXn, TNx, and TNn) are higher than others.

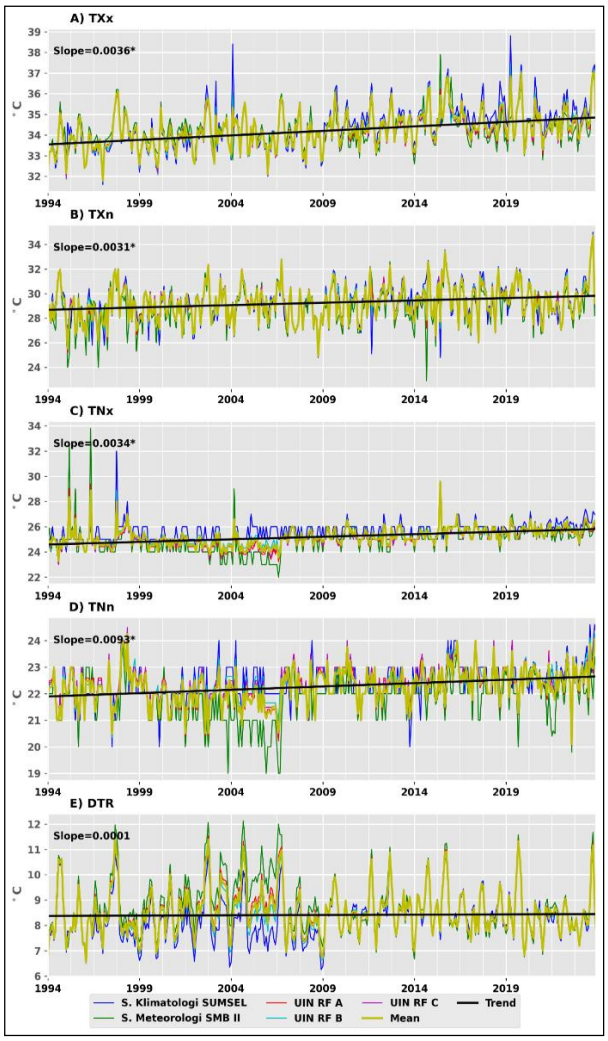

Figure 2. Extreme temperature time series. The black line is the trend, while * depicts the significance level at 95%.

Table 2. Variances of time-series of extreme temperatures at the focus of locations

Focus of locations	TXx	TXn	TNx	TNn	DTR
S. Klimatologi SUMSEL	1.12	2.30	0.57	0.57	0.82
S. Meteorologi SMB II	0.71	2.55	1.29	0.76	1.17
UIN RF A	0.75	2.12	0.63	0.49	0.90
UIN RF B	0.85	2.09	0.47	0.47	0.82
UIN RF C	0.77	2.09	0.57	0.48	0.87

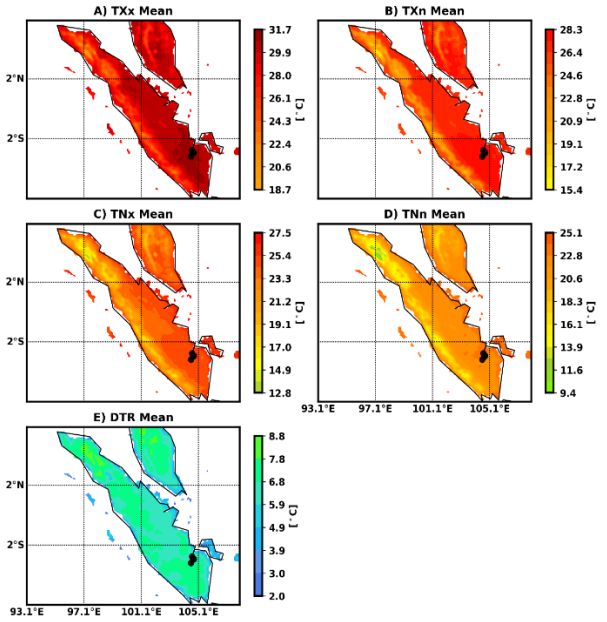

Figure 3. The Means of extreme temperatures. A, B, C, D, and E heatmap the means of TXx, TXn, TNx, TNn, and DTR, respectively, over 30 years

As shown in Table 3, the total variance calculated up to the 15th EOF ranges from 83.45% to 95.23%. This total variance shows that the EOF can cover almost all of the variability of each extreme temperature. The first two largest variabilities are EOF1 and EOF2, which respectively range within 46.81%-56.93% and 11.27%-26.15%. Even though the total variance of DTR is the highest, at EOF1, the largest variance is actually in TXx. This shows that each EOF can cover different temperature variability. Because the variance of EOF1 and EOF2 is relatively larger than those of the other EOFs, we only display the spatial EOF results for EOF1 and EOF2, shown in Figure 4.

The EOF1 results in Figure 4 show low extreme temperature variability in the Sumatra region. In EOF1 of TXx (Figure 4.A), it can be seen that there are two dominant extreme temperature areas in Sumatra, namely the coastal area and the central part. The coastal area shows higher TXx than the central part. Based on Figure 4.B, it can be seen that the TXx amplitude fluctuates throughout the observation years, especially around 2000-2017. Interestingly, a very weak amplitude was detected in 2018-2023, although what caused this is not yet known. However, closer observation of Figure 2.A indicates a decline in TXx starting at the end of 2019 and continuing until 2023. This means that since 2019, TXx has tended to decline,

Table 3. Variances (%) of extreme temperatures by EOF components. Total variance covered by the EOF is the sum from first to fifteenth component, but we show only five components because the sixth until fifteenth are too small to matter.

Extreme temperature index	Variance covered by EOF	EOF 1	EOF 2	EOF 3	EOF 4	EOF 5
TXx	89.23	56.93	12.80	5.28	4.02	2.43
TXn	84.2	47.85	13.60	5.18	4.62	2.26
TNx	83.46	54.97	11.27	5.57	2.93	1.63
TNn	83.45	46.96	19.44	3.59	2.57	1.85
DTR	95.23	46.81	26.15	8.42	4.52	2.73

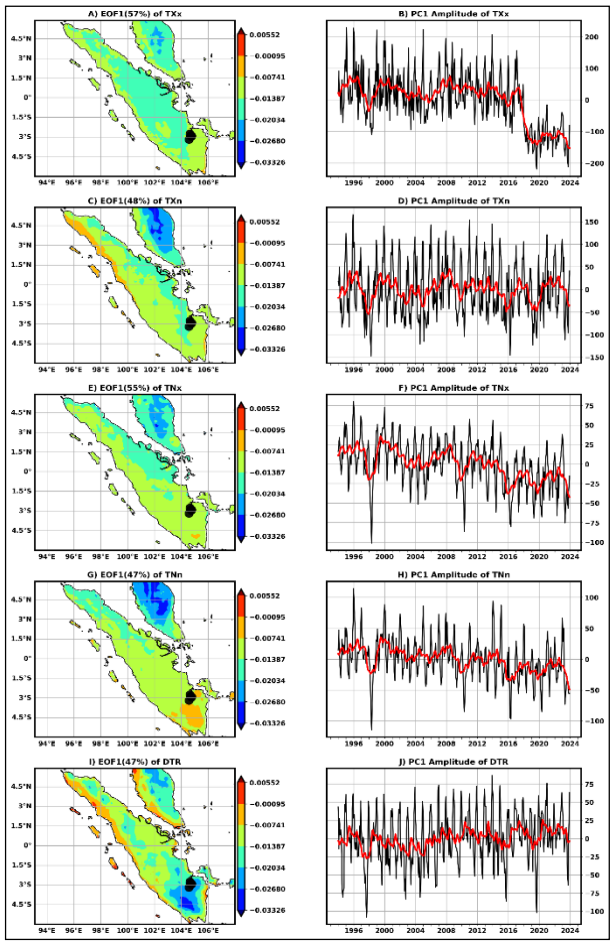

Figure 4. The EOF1 (left) and PC1 (right) of the extreme temperature indices (TXx, TXn, TNx, TNn, DTR). The red line is a smoothing approximation of PC amplitude.

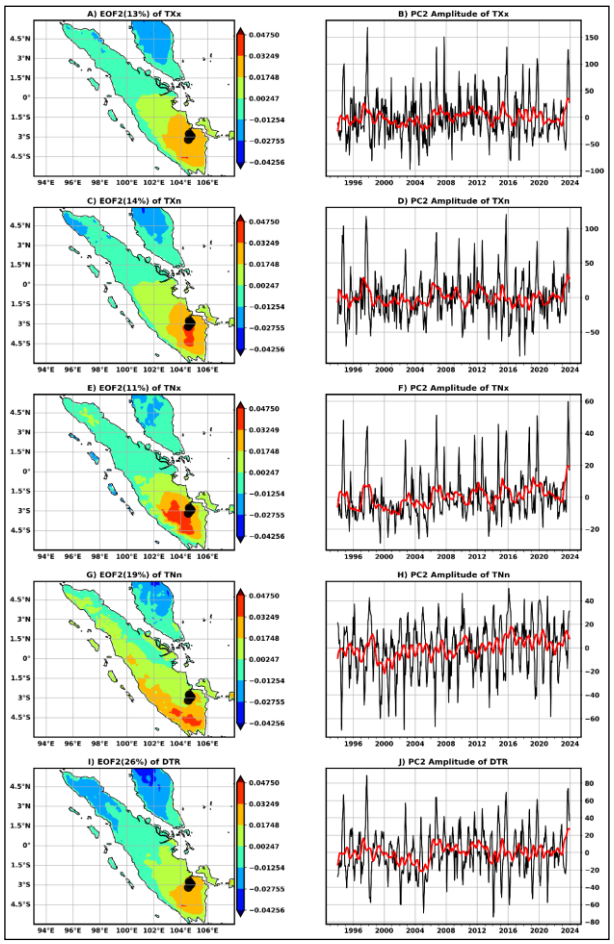

Figure 5. The EOF2 (left) and PC2 (right) of the extreme temperature indices (TXx, TXn, TNx, TNn, DTR). The red line is a smoothing approximation of PC amplitude.

although further studies regarding this situation need to be carried out. Based on Figure 4.C, at least three TXn regions can be seen. The area with the highest TXn variability is on the western coastline of the northern part of Sumatra, precisely at latitudes 0°-6°N. Next, the area with wider TXn variability is in the central part, then along the east coast of Sumatra. In addition, the TXn amplitude (Figure 4.D) fluctuates regularly. This shows that TXn fluctuations are relatively constant throughout the observation years. TNx variability (Figure 4.E) based on EOF1 is at least separated into two regions, namely most of the west coast of the northern region to all of southern Sumatra. In general, TNn variability (Figure 4.G) based on EOF1 also shows the same distribution pattern; only the distribution of TNn at higher temperatures is wider than of TNx. This shows that throughout the year, observations of minimum nighttime temperatures have increased. This condition is also indicated by the amplitude of TNn (Figure 4.H), which is flatter than TNx (Figure 4.F). EOF1 shows that DTR (Figure 4.I) in southern Sumatra, especially FoL, is lower than elsewhere. However, the DTR amplitude on PC1 (Figure 4.J) shows a relatively constant condition.

As can be seen in Table 3, the EOF2 variability of extreme temperatures covers a variance of 11.27%-26.15%, and spatially is shown in Figure 5. In general, EOF2 has a higher variability of extreme temperatures than EOF1. The TXx variability based on EOF2 (Figure 5.A) shows a higher temperature distribution in the southern region than in other regions, including FoL. The same pattern also occurs in TXn (Figure 5.C) and TNx (Figure 5.E). However, TNn areas with higher temperatures (Figure 5.G) are more widely distributed than those with lower temperatures. Apart from that, DTR variability (Figure 5.I) based on EOF2 also shows that extreme temperatures in the southern region are higher than in other regions.

The PC2 amplitude of each extreme temperature (Figure 5.B, Figure 5.D, Figure 5.F, Figure 5.H, Figure 5.J) shows a corresponding pattern, especially between TXx and TXx, TNx and TNn. The EOF2 results, based on the PC2 of each extreme temperature index, are also more consistent with several ENSO events. For example, several high TXx and TXn amplitudes occurred simultaneously with El Niño (in 1997 and 2015). Furthermore, the highest TNx occurred in 2023, along with a positive IOD.

As shown in Figures 4 and 5 (B, D, F, H, and J), each extreme temperature index PC amplitude fluctuates so much that it is difficult to detect periods of recurrence. Therefore, analysis was carried out using FFT to see the recurring period of these events, and the results are shown in Figure 6. These

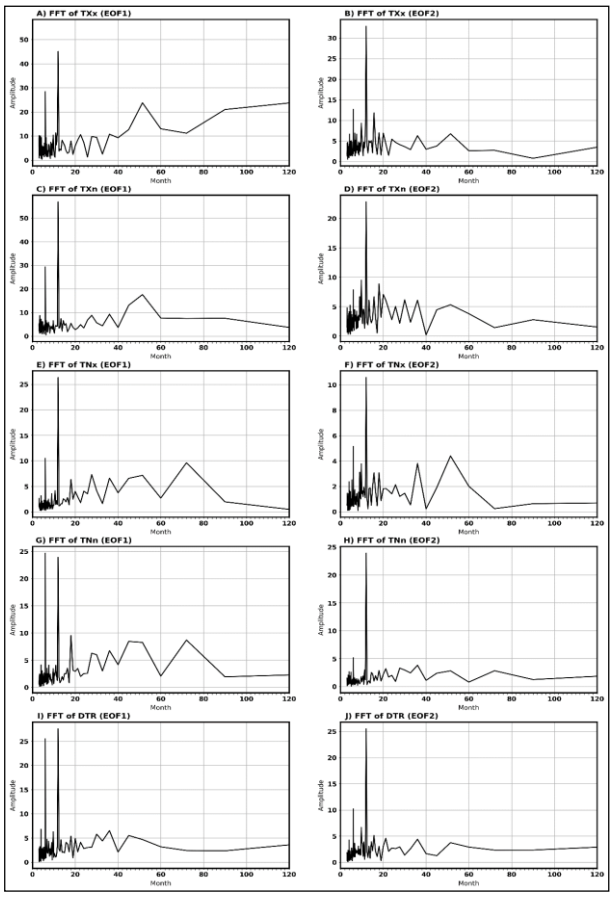

Figure 6. FFT of EOF1 (left) and EOF (right) of the extreme temperatures (TXx, TXn, TNx, TNn, DTR)

results (Figure 6.A-J) show that the peaks of each extreme temperature based on EOF1 occur every 6 months and 12 months (Figure 6.A, Figure 6.C, Figure 6.E, Figure 6.G, and Figure 6.I). Furthermore, each extreme temperature peak based on EOF2 occurs every 12 months (Figure 6.B, Figure 6.D, Figure 6.F, Figure 6.H, and Figure 6.J). This annual cycle of extreme temperatures coinciding with El Niño and positive IOD was also shown in the study of Dittus *et al.* (2018).

4. Conclusions

Evaluation of extreme temperatures in FoL shows an increasing trend over the last 30 years (1994-2023). This increasing trend indicates that the last maximum temperature in FoL at night is the same as the minimum temperature during the day was initially. In general, EOF1 shows that the distribution of warmer temperatures at minimum temperatures (TXn and TNn) is wider than at maximum temperatures (TXx and TNx). EOF1 also shows that extreme temperatures in FoL are always higher than in other regions. Meanwhile, the extreme temperature variability shown based on EOF2 is higher than that of EOF1, although with a lower variance coverage. EOF2 also shows that warmer extreme temperatures occur in southern Sumatra, including at FoL. In addition, in mode 2, PC shows amplitude peaks detected in the ENSO and IOD (El Niño and positive IOD) periods.

Acknowledgements

This study is part of Penelitian Berbasis Standar Biaya Keluaran Universitas Islam Negeri Raden Fatah Palembang, NOMOR 779 TAHUN 2024, Fiscal Year 2024, with Registration ID: 241090000090723.

References

Akbar, A. J., & Lubis, A. M. (2022). Analysis of land and sea temperatures trend during 1985-2021 period to understand local or global warming effect in Bengkulu city. *Indonesian Review of Physics*, *5*(1), 16–24. Retrieved from https://doi.org/10.12928/irip.v5i1.6073

Akhsan, H., Irfan, M., & Iskandar, I. (2023). El Niño Southern Oscillation (ENSO), Indian Ocean Dipole (IOD), and the rise of extreme temperatures in eastern Sumatra: Exploring climate change dynamics. *Jurnal Penelitian Pendidikan IPA*, *9*(2), 600–608. Retrieved from https://doi.org/10.29303/jppipa.v9i2.3084

Akhsan, H., Romadoni, M., & Ariska, M. (2022). Prediction of extreme temperature in south Sumatra and its applications at the end of the 21st century. *Jurnal Penelitian Pendidikan IPA*, *8*(2). Retrieved from https://doi.org/10.29303/jppipa.v8i2.1363

An, D., Du, Y., Berndtsson, R., Niu, Z., Zhang, L., & Yuan, F. (2020). Evidence of climate shift for temperature and precipitation extremes across Gansu Province in China. *Theoretical and Applied Climatology*, *139*(3–4), 1137–1149. Retrieved from https://doi.org/10.1007/s00704-019-03041-1

Antonio, N., & Valeria, S. (2010). *A guide to empirical orthogonal functions for climate data analysis*. Berlin/Heidelberg, Germany: Springer.

Chaney, N. W., Sheffield, J., Villarini, G., & Wood, E. F. (2014). Development of a high-resolution gridded daily meteorological dataset over sub-Saharan Africa: Spatial analysis of trends in climate extremes. *Journal of Climate*, *27*(15), 5815–5835. Retrieved from https://doi.org/10.1175/JCLI-D-13-00423.1

Choi, G., Collins, D., Ren, G., Trewin, B., Baldi, M., Fukuda, Y., Zhou, Y. (2009). Changes in means and extreme events of temperature and precipitation in the Asia-Pacific Network region, 1955-2007. *International Journal of Climatology*, *29*(13), 1906–1925. Retrieved from https://doi.org/10.1002/joc.1979

Dittus, A. J., Karoly, D. J., Donat, M. G., Lewis, S. C., & Alexander, L. V. (2018). Understanding the role of sea surface temperature-forcing for variability in global temperature and precipitation extremes. *Weather and Climate Extremes*, *21*, 1–9. Retrieved from https://doi.org/10.1016/J.WACE.2018.06.002

Felix, M. L., Kim, Y. K., Choi, M., Kim, J. C., Do, X. K., Nguyen, T. H., & Jung, K. (2021). Detailed trend analysis of extreme climate indices in the upper geum river basin. *Water (Switzerland)*, *13*(22). Retrieved from https://doi.org/10.3390/w13223171

Feng, T., Tipton, Z., Xia, L., & Chang, Y. (2019). Evaluation of CORDEX regional climate models in simulating extreme dry spells in southwest China. *Frontiers in Earth Science*, *7*, 294. Retrieved from https://doi.org/

10.3389/feart.2019.00294

Hannachi, A., Jolliffe, I. T., & Stephenson, D. B. (2007). Review empirical orthogonal functions and related techniques in atmospheric science: A review. *International Journal of Climatology*, *27*(May 2007), 1119–1152. Retrieved from https://doi.org/10.1002/joc

IPCC. (2012). *Managing the risks of extreme events and disasters to advance climate change adaptation. A special report of working groups I and II of the Intergovernmental Panel on Climate Change [Field, C.B., V. Barros, T.F. Stocker, D. Qin, D.J. Dokken, K.L. Ebi, M.D.]* Cambridge, England: Cambridge University Press.

IPCC. (2018). *IPCC Special Report on the impacts of global warming of 1.5°C*. Cambridge, England: Cambridge University Press.

Iskandar, I., Sari, Q. W., Setiabudiday, D., Yustian, I., & Monger, B. (2017). The distribution and variability of chlorophyll-a bloom in the southeastern tropical Indian ocean using empirical orthogonal function analysis. *Biodiversitas*, *18*(4), 1546–1555. Retrieved from https://doi.org/10.13057/biodiv/d180433

Khoir, A. N., Mamlu'Atur, R., Safril, A., & Fadholi, A. (2018). Analysis of changes in daily temperature and precipitation extreme in Jakarta on period of 1986-2014. *MATEC Web of Conferences*, *229*. Retrieved from https://doi.org/10.1051/matecconf/201822902017

Limjirakan, S., & Limsakul, A. (2012). Observed trends in surface air temperatures and their extremes in Thailand from 1970 to 2009. *Journal of the Meteorological Society of Japan*, *90*(5), 647–662. Retrieved from https://doi.org/10.2151/jmsj.2012-505

Nie, H., Qin, T., Yang, H., Chen, J., He, S., Lv, Z., & Shen, Z. (2019). Trend analysis of temperature and precipitation extremes during winter wheat growth period in the major winter wheat planting area of China. *Atmosphere*, *10*(5). Retrieved from https://doi.org/10.3390/atmos10050240

Stott, P. A., Christidis, N., Otto, F. E. L., Sun, Y., Vanderlinden, J. P., van Oldenborgh, G. J., . . . Zwiers, F. W. (2016). Attribution of extreme weather and climate-related events. *Wiley Interdisciplinary Reviews: Climate Change*, *7*(1), 23–41. Retrieved from https://doi.org/10.1002/wcc.380

Subarna, D. (2017). Analysis of long-term temperature trend as an urban climate change indicator. *Forum Geografi*, *31*(2), 196–208. Retrieved from https://doi.org/10.23917/forgeo.v31i2.4189

Supari, Tangang, F., Juneng, L., & Aldrian, E. (2017). Observed changes in extreme temperature and precipitation over Indonesia. *International Journal of Climatology*, *37*(4), 1979–1997. Retrieved from https://doi.org/10.1002/joc.4829

Zhang, X., Feng, Y., & Chan, R. (2018). Introduction to RClimDex v1.9. *Climate Research Division Environment Canada*, 1–26. Retrieved from https://usermanual.wiki/Document/manual.2056401896.pdf